*Ferroelectrics*, 400:3–7, 2010

ISSN: 0015-0193 print / 1563-5112 online
DOI: 10.1080/00150193.2010.505521

Taylor & Francis
Taylor & Francis Group

# Ferromagnetism and Spin-Glass-Like Behavior of $BiFeO_3$ Nanoparticles

J. ZHONG,[1,2] J. J. HEREMANS,[3] DWIGHT VIEHLAND,[1,2]
G. T. YEE,[4] AND S. PRIYA[1,2,*]

[1]Center for Energy Harvesting Materials and Systems, Virginia Tech, Blacksburg, Virginia 24061, USA
[2]Department of Materials Science and Engineering, Department of Mechanical Engineering, Virginia Tech, Blacksburg, Virginia 24061, USA
[3]Department of Physics, Virginia Tech, Blacksburg, Virginia 24061, USA
[4]Department of Chemistry, Virginia Tech, Blacksburg, Virginia 24061, USA

*$BiFeO_3$ (BFO) nanoparticles were synthesized by the sol-gel method. X-ray diffraction and energy dispersive X-ray spectroscopy indicate no secondary phases are present, and the composition of the $BiFeO_3$ nanoparticles was stoichiometric. Magnetic measurements show that the $BiFeO_3$ nanoparticles exhibit ferromagnetism with spin-glass-like behavior. The results were found to be related to size effects, which partially destroy the long-wavelength cycloid spin structure, and which induce ferromagnetism and spin-glass-like behavior due to diffusion of domain walls and pinning at the nanoparticle surface.*

**Keywords** Bismuth ferrite; nanoparticles; ferromagnetic; multiferroic

Multiferroics show coupled electric, magnetic, and structural orders, in the simultaneous presence of ferroelectricity, ferromagnetism, and ferroelasticity. Multiferroic materials offer wide opportunities for potential applications in information storage and in spintronic devices and sensors, where the coupling between electric and magnetic polarizations can be used for new functionalities [1]. The perovskite $BiFeO_3$ (BFO) shows multiferroicity, and in bulk form possesses both high ferroelectric Curie temperature $T_C = 1143$ K and high antiferromagnetic Néel temperature $T_N = 643$ K [2]. BFO displays G-type antiferromagnetism, wherein the $Fe^{3+}$ magnetic moments are coupled ferromagnetically within the (111) planes and antiferromagnetically between neighboring planes [3, 4]. The presence of $Fe^{3+}$ ions on the B-site in antiferromagnetic ordering was confirmed by neutron diffraction, with a magnetic moment of $\mu_{Fe} = 3.70\ \mu_B$ [5, 6]. Further, it was found using high resolution neutron powder diffraction that the BFO structure could be described with almost similar accuracy using modulated magnetic ordering models such as a circular cycloid, an elliptical cycloid and a spin density wave [7]. Superimposed on the antiferromagnetic order a cycloidal spatially modulated spin structure is present in bulk samples, responsible

Received in final form October 7, 2009.
*Corresponding author. E-mail: spriya@vt.edu

for a cancellation of the macroscopic magnetization [8]. The axis of spin alignment precesses through the crystal, and the resulting helical spin structure has a long wavelength, of 62 nm, incommensurate with the lattice spacing [9, 10]. The cycloidal spin modulation is thought to result in zero linear magnetoelectric coupling in single-crystals; however, it could be absent in strained films or nanoparticles. As a result, weak ferromagnetism has been suggested experimentally [11–14], and also theoretically predicted [8], in thin films.

Current research on understanding the magnetic behavior of BFO is focused on bulk materials and thin films with few results published on nanoparticles. It is recognized that size effects can induce unique phenomena and provide information to help elucidate fundamental material behavior. For example, the spin structure in constrained BFO thin films appears to differ from that of bulk BFO, where the cycloidal spin modulation may be absent due to strain. Thus, our focus lies on understanding the magnetic behavior of the BFO nanoparticles obtained in this work.

The BFO nanoparticles were synthesized by the sol-gel method. Bismuth nitrate ($Bi(NO_3)_3{\cdot}5H_2O$) and iron nitrate ($Fe(NO_3)_3{\cdot}9H_2O$) in stoichiometric proportions (1:1 molar ratio) were dissolved in 2-methoxyethanol ($C_3H_8O_2$). The solution was adjusted to a pH value of 4–5 by adding 2-methoxyethanol and nitric acid. This mixture was stirred for 30 minutes at room temperature to obtain the sol, which was then kept at 80°C for 96 hours to form the dried gel powder. The dried powder was calcined in temperature range of 400–600°C for 1–3 h in air. The optimal calcination temperature and time for the BFO nanoparticles reported on here, was 450°C for 2 hours. The structure and morphology of BFO nanoparticles were investigated by powder X-ray diffraction (XRD), and scanning electron microscopy (SEM). For magnetic measurements, superconducting quantum interference device (SQUID) magnetometry was used.

Figure 1 contains the XRD pattern of the synthesized BFO nanoparticles, for which a single-phase perovskite structure is apparent. The (111) peak-splitting indicate a rhombohedral structure for the nanoparticles, consistent with the reported structure of BFO ceramics [15]. A SEM micrograph of a BFO nanoparticle assembly is depicted in Fig. 2, revealing a spherical morphology with average particle size of 20 nm.

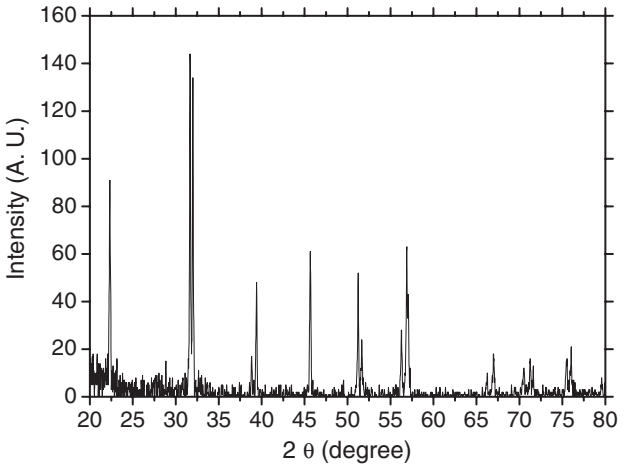


**Figure 1.** Powder X-ray diffraction pattern of the as-synthesized $BiFeO_3$ nanoparticles.

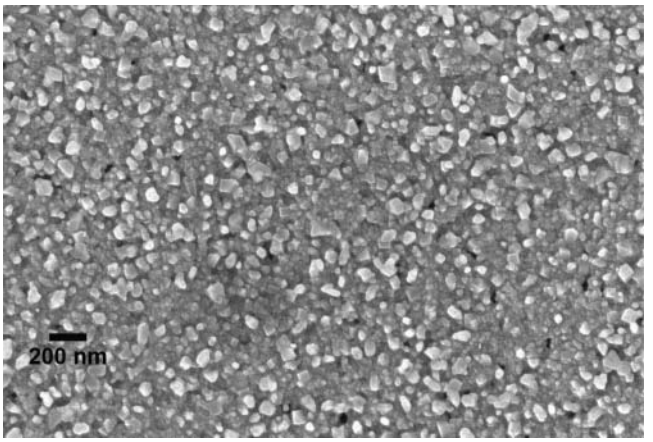


**Figure 2.** Scanning electron micrograph of the $BiFeO_3$ nanoparticles.

Figure 3 shows the magnetic field ($H$) dependence of the magnetization ($M$) for the BFO nanoparticles at temperatures ($T$) of 10 K, 77 K and 298 K. The magnetic hysteresis shows that the BFO nanoparticles exhibit ferromagnetic properties from 10 K to room temperature. As mentioned above, in bulk BFO single crystals the magnetization measurements are expected to exhibit antiferromagnetic response without any trace of weak ferromagnetism [16, 17]. Yet, weak ferromagnetism is often reported in polycrystalline BFO ceramics and thin films, sometimes imputed to the presence of small traces of magnetic impurities [18]. An observed spontaneous magnetization in as-synthesized BFO samples has also been ascribed to cumulative effects of mixed $Fe^{2+}/Fe^{3+}$ valence formation, of suppression of the helical spin structure, of an increase in canting angle, and/or of iron-rich nanoclusters [11, 12, 14, 15, 19–21]. A spin-glass behavior has also been observed in the $M$ ($T$) and $M$ ($H$) measurements for BFO films annealed in air atmosphere, further enhanced by annealing

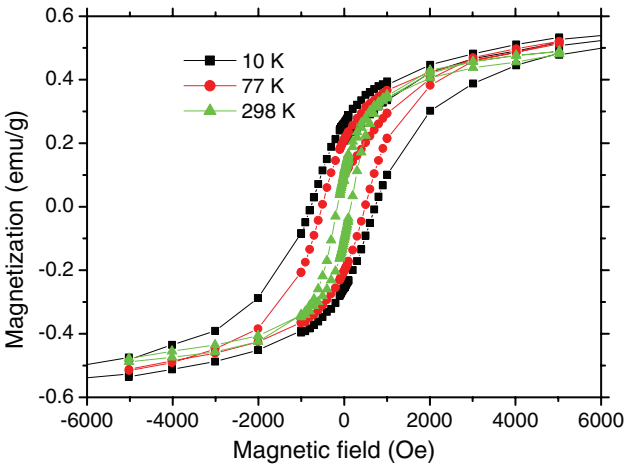


**Figure 3.** Magnetic field dependence of the magnetization for the $BiFeO_3$ nanoparticles at 10 K, 77 K and 298 K. (See Color Plate I)

**Table 1**
Energy dispersive X-ray spectroscopy analysis of $BiFeO_3$ nanoparticles

| Element | Atomic % | Uncert. % | Correction | k-Factor |
|---|---|---|---|---|
| Fe(K) | 50.28 | 2.97 | 0.99 | 1.451 |
| Bi(L) | 49.71 | 4.50 | 0.75 | 6.708 |

the sample in an oxygen atmosphere and hence tentatively related to the formation of iron oxide nanoclusters or precipitates [14, 21]. In our case, the observed ferromagnetism can be attributed to a size effect resulting from the nanoparticle geometry. Indeed, according to the XRD and EDS analysis contained in Table I, no secondary phases are present, and the BFO nanoparticle composition was stoichiometric. Therefore, we impute the observation of ferromagnetism to nanoparticle size factors influencing the spin structure. The wavelength of the fully developed incommensurate cycloid spin structure in bulk BFO is 62 nm [22], larger than the scale of our BFO nanoparticles. So, the spin structure characteristic of antiferromagnetic bulk BFO is interrupted by the particle surface in the BFO nanoparticles, an effect that in thin films can be conducive to ferromagnetic behavior [14, 17].

Figure 4 shows the dependence on $T$ of the magnetization $M$ ($T$) under zero-field-cooled (ZFC) and field-cooled (FC) conditions. The $M$ ($T$) was measured under applied $H$ of 5000 Oe. At 5000 Oe the saturation magnetization is not reached, as can be observed in Fig. 3. Yet, the low-$T$ value for the magnetization measured in the present work, $\sim$0.52 emu/g, is comparable to the $\sim$ 0.49 emu/g recently measured in nanocrystalline films under FC conditions [23]. $M$ ($T$) in Fig. 4 moreover shows irreversibility between FC and ZFC conditions over a wide range of $T$, a clear indication of spin-glass-like behavior and a common point with Ref. 23. For BFO, spin-glass-like behavior has been observed in both single-crystal and thin film samples (see *e.g.* [24]). However, Fig. 4 contains evidence of spin-glass-like behavior in BFO nanoparticles. The unique long-range spiral spin structure characteristic of bulk BFO will lead to spin-glass behavior differing from Ising systems. The spin-glass behavior may have long-range Coulumbic contributions to the

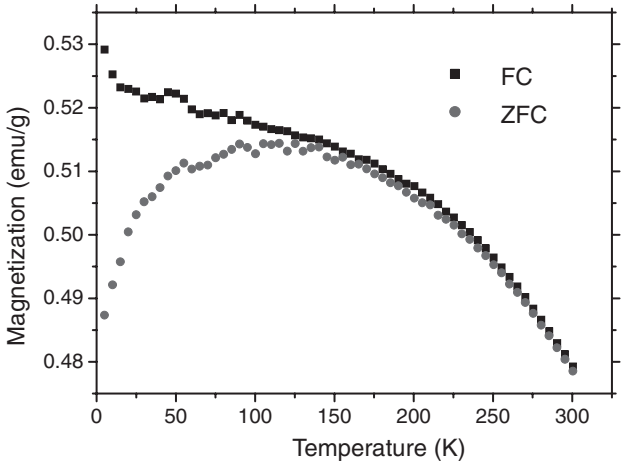


**Figure 4.** Temperature dependence of the magnetization for the $BiFeO_3$ nanoparticles at an applied magnetic field of 5000 Oe, in zero-field-cooled (ZFC) and field-cooled (FC) conditions.

electromagnons which are not pure spin waves [25]. Pinning of the incomplete spin spiral structure at the nanoparticle boundaries may also result in the experimental observation of spin-glass-like $M$ ($T$). Further, spin-glass-like behavior in BFO has been ascribed to diffusion of domain walls, since the domain walls in BFO are known to influence both ferroelectric and ferromagnetic properties [26].

In summary, both ferromagnetic properties and spin-glass-like behavior were observed in BFO nanoparticles. Ferromagnetic behavior has been ascribed to a partial destruction in nanoparticles of the long-wavelength cycloid spin structure expected in bulk BFO. Spin-glass-like behavior has been imputed to diffusion of domain walls, with possible contributions from pinning of the cycloid spin structure at the nanoparticle surface.

## Acknowledgments

This research was sponsored by Virginia Tech's Institute for Critical Technologies and Applied Sciences (ICTAS) and by AFOSR.

## References

1. T. Zhao, A. Scholl, F. Zavaliche, K. Lee, M. Barry, A. Doran, M. P. Cruz, Y. H. Chu, C. Ederer, N. A. Spaldin, R. R. Das, D. M. Kim, S. H. Baek, C. B. Eom, and R. Ramesh, *Nature Materials* **5**, 823 (2006).
2. J. M. Moreau, C. Michel, R. Gerson *et al.* , *J. Phys. Chem. Solids* **32**, 1315 (1971).
3. P. Fischer, M. Połomska, I. Sosnowska, and M. Szymański, *J. Phys. C: Solid St. Phys.* **13**, 1931 (1980).
4. R. Przenioslo, A. Palewicz, M. Regulsk, I. Sosnowska, R. M. Ibberson, and K. S. Knight, *J. Phys: Condens. Matter* **18**, 2069 (2006).
5. I. Sosnowska, R. Przenioslo, P. Fischer *et al.* , *Acta Phys Polonica A* **86**, 629 (1994).
6. I. Sosnowska, R. Przenioslo, P. Fischer, *et al.*, *J. Magn. Magn. Mater.* **160**, 384 (1996).
7. R. Przenioslo, M. Regulski, and I. Sosnowska, *Jpn. J. Phys. Soc.* **75**(8), 084718 (2006).
8. C. Ederer, and N. A. Spaldin, *Phys. Rev. B.* **71**, 060401 (2005).
9. A. V. Zalessky, A. A. Frolov, A. K. Zvezdin *et al.* , *J. Exp. Theor. Phys.* **95**, 101 (2002).
10. A. V. Zalessky, A. A. Frolov, T. A. Khimich, *et al. Europhys. Lett.* **50**, 547 (2000).
11. J. Wang, J. B. Neaton, H. Zheng, V. Nagarajan, S. B. Ogale, B. Liu, D. Viehland, V. Vaithyanathan, D. G. Schlom, U. V. Waghmare, N. A. Spaldin, K. M. Rabe, M. Wuttig, and R. Ramesh, *Science* **299**, 1719 (2003).
12. H. Naganuma and S. Okamura, *J. Appl. Phys.* **101**, 09M103 (2007).
13. H. Bea, M. Bibes, S. Petit, J. Kreisel, and A. Barthelemy, *Philos. Mag. Lett.* **87** 165 (2007).
14. P. K. Siwach, H. K. Singh, J. Singh, and O. N. Srivastava, *Appl. Phys. Lett.* **91**, 122503 (2007).
15. S. T. Zhang, M. H. Lu, D. Wu, Y. F. Chen, and N. B. Ming, *Appl. Phys. Lett.* **87**, 262907 (2005).
16. D. Lebeugle, D. Colson, A. Forget, *et al.*, *Phys Rev B* **76**, 024116 (2007).
17. F. M. Bai, J. L. Wang, M. Wuttig, *et al.*, *Appl. Phys. Lett.* **86**, 032511 (2005).
18. K. Takahashi, and M. Tonouchi, *J. Magn. Magn. Mater.* **310**, 1174 (2007).
19. J. B. Li, G. H. Rao, J. K. Liang, *et al.*, *Appl. Phys. Lett.* **90**, 162513 (2007).
20. W. Eerenstein, F. D. Morrison, J. Dho, *et al.*, *Science* **307**, 1203a (2005).
21. H. Béa, M. Bibes, S. Fusil, *et al.*, *Phys. Rev. B* **74**, 020101 (2006).
22. A. V. Zalesskii, A. K. Zvezdin, A. A. Frolov, and A. A. Bush, *JETP Lett.* **71**, 465 (2000).
23. S. Vijayanand, M. B. Mahajan, H. S. Potdar, and P. A. Joy, *Phys. Rev. B* **80**, 064423 (2009).
24. M. K. Singh, R. S. Katiyar, W. Prellier, and J. F. Scott, *J. Phys.: Cond. Matter* **21**, 042202 (2009).
25. Yu. G. Chukalkin and B. N. Goshchitskii, *Phys. Status Solidi A* **200**, R9 (2003).
26. G. Catalan, H. Bea, S. Fusil, M. Bibes, P. Paruch, A. Barthelemy, and J. F. Scott, *Phys. Rev. Lett.* **100**, 027602 (2008).